This equation is satisfied by the hypergeometric series, absolutely convergent for $|\theta| < 1$

$$F(a,b,c,\theta) = 1 + \frac{a\cdot b}{1\cdot c}\theta + \frac{a(a+1)b(b+1)}{1\cdot 2\cdot c(c+1)}\theta^2 + \frac{a(a+1)(a+2)b(b+1)(b+2)}{1\cdot 2\cdot 3\cdot c(c+1)(c+2)}\theta^3 + \ldots \quad (16)$$

where

$$a = \tfrac{3}{2}, \quad b = -\tfrac{1}{2}, \quad c = \tfrac{5}{2} \quad (17)$$

From the definition (10) or (11) of $\phi$, it is seen that when $E$ or $H = 0$, $\theta = 0$, $\phi = 0$, and $d\phi/d\theta = 1$. Hence the solution of Eq. (15) satisfying these conditions is

$$\phi = \tfrac{10}{3} - \tfrac{10}{3}F(\tfrac{3}{2}, -\tfrac{1}{2}, \tfrac{5}{2}, \theta) \quad (18)$$

Explicitly, we have

$$\phi = \theta + \frac{5}{28}\theta^2 + \frac{5}{72}\theta^3 + \frac{25}{704}\theta^4 + \ldots + \frac{5\cdot 1\cdot 3\cdot 5\ldots(2n-3)}{n(2n+3)\cdot 2\cdot 4\cdot 6\ldots(2n-2)}\theta^n + \ldots \quad (19)$$

The recurrence formula for computing the coefficient $a_n$ of $\theta^n$ of this series is

$$a_n = \frac{(2n+1)(2n-3)}{2n(2n+3)}a_{n-1} \quad (20)$$

Reversing the series

$$\theta = \phi - \frac{5}{28}\phi^2 - \frac{5}{882}\phi^3 - \frac{1075}{543312}\phi^4 - \ldots \quad (21)$$

Since $\theta = (1-e)/2$ in both the elliptic and the hyperbolic case, we have the final series for the eccentricity valid for either the elliptic or the hyperbolic orbit.

$$e = 1 - 2\phi + \frac{5}{14}\phi^2 + \frac{5}{441}\phi^3 + \frac{1075}{271656}\phi^4 + \ldots \quad (22)$$

By the convergent property of the hypergeometric function, it is seen that the series is absolutely convergent when $|\theta| < 1$, that is, for

$$e < 3 \quad (23)$$

### References

[1] Whittaker, E. T. and Watson, G. N., *A Course of Modern Analysis*, Cambridge University Press, New York, 1963, pp. 281–283.

# Vibrations of Sandwich Plates under Uniaxial Compression

Y. V. K. Sadasiva Rao* and P. K. Sinha*
*Vikram Sarabhai Space Centre, Trivandrum, India*

### Introduction

Vibrations of sandwich plates have been investigated by many authors.[1] Most of the papers that appear in the literature restrict the analysis either to symmetric sandwich plates (having identical faces), or to plates taking the membrane energy of the faces alone. Among earlier investigators, Hoff[2] first included the bending rigidity of the faces for studying the bending and buckling behavior of symmetric sandwich plates. Recently, Rao and Nakra[3] considered the effects of the bending rigidity of the faces as well as rotary, longitudinal translatory, and transverse inertias in their analysis for the case of free vibrations of sandwich plates with dissimilar faces. However, the influence of edge forces on the vibrations of a sandwich plate has not been studied in detail. To the authors' knowledge, only Shahin[4] presented a few results on the free vibrations of sandwich plates in the presence of mostly in-plane tensile loads treating the faces as membranes. The results are inadequate, as they fail to identify the behavior of the plate, particularly when the edge loads are compressive in nature.

A detailed study of the dynamic behavior of unsymmetric sandwich plates (having dissimilar faces) under uniaxial compression, taking the bending energy of the faces into account, has been presented in this Note. The effect of variation of various nondimensional parameters has also been investigated.

Received December 27, 1973; revision received April 5, 1974.
Index category: Structural Dynamic Analysis.
* Engineer, Structural Engineering Division.

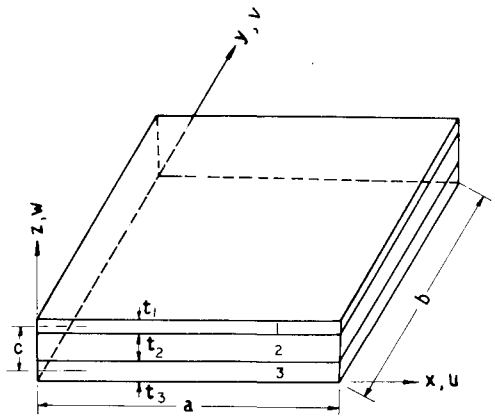


**Fig. 1 Geometry of sandwich plate.**

### Governing Equations and Solution

As an extension of Ref. 3, one can obtain the equations of motion for the vibrations of an unsymmetrical sandwich plate (Fig. 1) under uniaxial compression accounting for the inertia term only. These are presented below:

$$S_1\left(u_1'' + \frac{1+\nu_1}{2}v_1'^* + \frac{1-\nu_1}{2}u_1^{**}\right) + \frac{S_2}{t_2^2}(cw' - u_1 + u_3) = 0 \quad (1)$$

$$S_1\left(v_1^{**} + \frac{1+\nu_1}{2}u_1'^* + \frac{1-\nu_1}{2}v_1''\right) + \frac{S_2}{t_2^2}(cw^* - v_1 + v_3) = 0 \quad (2)$$

$$S_3\left(u_3'' + \frac{1+\nu_3}{2}v_3'^* + \frac{1-\nu_3}{2}u_3^{**}\right) - \frac{S_2}{t_2^2}(cw' - u_1 + u_3) = 0 \quad (3)$$

$$S_3\left(v_3^{**} + \frac{1+\nu_3}{2}u_3'^* + \frac{1-\nu_3}{2}v_3''\right) - \frac{S_2}{t_2^2}(cw^* - v_1 + v_3) = 0 \quad (4)$$

$$(D_1 + D_3)\nabla^4 w - S_2\frac{c}{t_2^2}\{c(w'' + w^{**}) - (u_1' + u_3' - v_1^* + v_3^*)\} + \rho\ddot{w} - N_x w'' = 0 \quad (5)$$

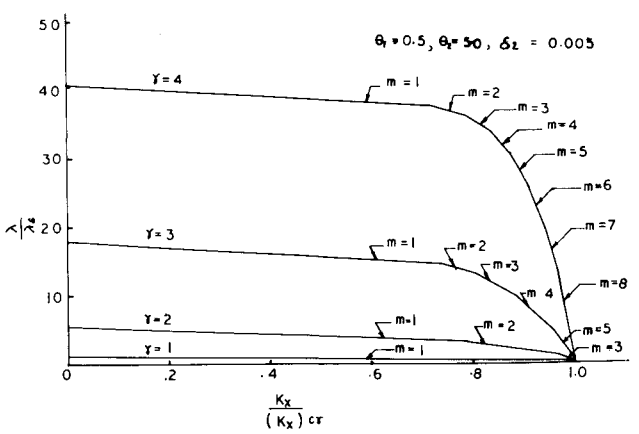


**Fig. 2 Variation of frequency ratio with axial load ratio.**

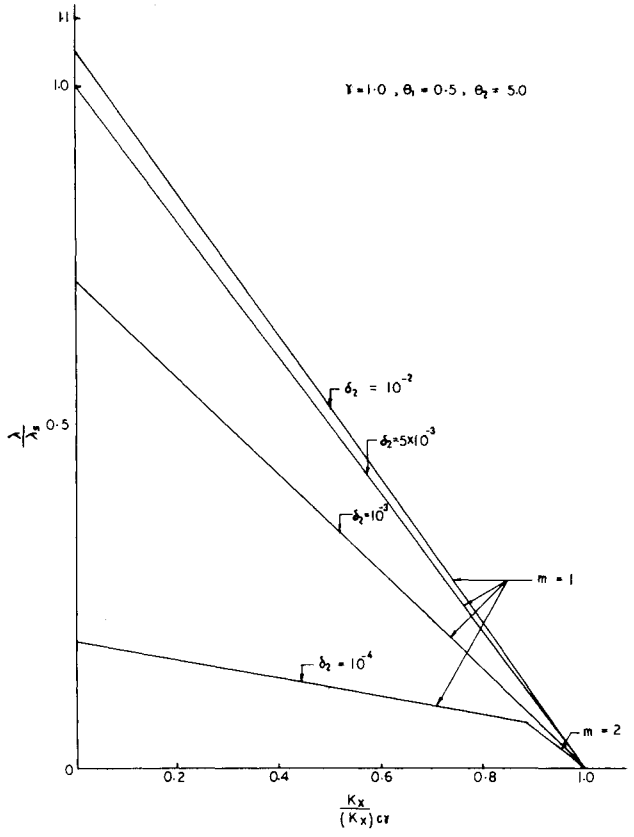


**Fig. 3 Variation of frequency ratio with axial load ratio.**

where

$$S_i = [E_i t_i/(1-\nu_i^2)](i = 1,3); \quad S_2 = G_2 t_2$$

$$D_i = [E_i t_i^3/12(1-\nu_i^2)](i = 1,3); \quad \rho = \rho_1 t_1 + \rho_2 t_2 + \rho_3 t_3$$

$E_i$, $\rho_i$, and $\nu_i$ are the Young's modulus, density, and Poisson's ratio of the layer $i$, respectively, $G_2$ is the transverse shear modulus of the core, and $N_x$ represents the applied compressive stress resultant. Subscripts 1 and 3 correspond to the face layers and 2, the core; a prime denotes differentiation with respect to $x$ and a star that with respect to $y$.

The boundary conditions for the case of a plate simply supported all along the edges are:

| along $x = 0, a$ | along $y = 0, b$ |
|---|---|
| i) $u_1' + \nu_1 v_1^* = 0$ | vii) $v_1^* + \nu_1 u_1' = 0$ |
| ii) $v_1' + u_1^* = 0$ | viii) $v_1' + u_1^* = 0$ |
| iii) $u_3' + \nu_3 v_3^* = 0$ | ix) $v_3^* + \nu_3 u_3' = 0$ |
| iv) $v_3' + u_3^* = 0$ | x) $v_3' + u_3^* = 0$ |
| v) $w = 0$ | xi) $w = 0$ |
| vi) $D_1(w'' + \nu_1 w^{**}) +$ $D_3(w'' + \nu_3 w^{**}) = 0$ | xii) $D_1(w^{**} + \nu_1 w'') +$ $D_3(w^{**} + \nu_3 w'') = 0$ |

(6)

It is already shown that conditions ii, iv, viii, and x of Eq. (6) need not be satisfied[2] and hence the following distributions for $u_1$, $u_3$, $v_1$, $v_3$, and $w$ are satisfied.

$$\begin{Bmatrix} u_1 \\ u_3 \end{Bmatrix} = \sum_{m=1}^{\infty}\sum_{n=1}^{\infty} \begin{Bmatrix} U_{1mn} \\ U_{3mn} \end{Bmatrix} \cos\frac{m\pi x}{a} \sin\frac{n\pi y}{b} \sin\omega t$$

$$\begin{Bmatrix} v_1 \\ v_3 \end{Bmatrix} = \sum_{m=1}^{\infty}\sum_{n=1}^{\infty} \begin{Bmatrix} V_{1mn} \\ V_{3mn} \end{Bmatrix} \sin\frac{m\pi x}{a} \cos\frac{n\pi y}{b} \sin\omega t \qquad (7)$$

and

$$w = \sum_{m=1}^{\infty}\sum_{n=1}^{\infty} W_{mn} \sin\frac{m\pi x}{a} \sin\frac{n\pi y}{b} \sin\omega t$$

where $\omega$ is the circular frequency in rad/sec.

Substitution of Eq. (7) in Eqs. (1–5) results in a set of simultaneous equations which can be written in the form:

$$\begin{aligned}
&U_{1mn} d_2 - U_{3mn} d_3 + V_{1mn} d_4 - W_{mn} d_1 = 0 \\
&-U_{1mn} d_3 + U_{3mn} f_2 + V_{3mn} f_3 - W_{mn} f_1 = 0 \\
&U_{1mn} d_4 + V_{1mn} e_2 - V_{3mn} d_3 - W_{mn} e_1 = 0 \\
&U_{3mn} f_3 - V_{1mn} d_3 + V_{3mn} g_2 - W_{mn} g_1 = 0 \\
&-U_{1mn} d_1 - U_{3mn} f_1 - V_{1mn} e_1 - V_{3mn} g_1 + W_{mn} h_1 = 0
\end{aligned} \qquad (8)$$

where

$$d_1 = \delta_2\left(1 + \frac{\theta_1}{2\theta_2}\right)$$

$$d_2 = \frac{\alpha_1\theta_1}{1-\psi_1^2\nu_3^2}\left\{m\beta + \frac{1-\psi_1\nu_3}{2}\gamma^2\beta\frac{n^2}{m}\right\} + d_3$$

$$d_3 = \frac{\delta_2}{\theta_2\beta m}; \quad d_4 = \frac{\alpha_1 n\theta_1\beta\gamma}{2(1-\psi_1\nu_3)}; \quad e_1 = \frac{n}{m}\gamma d_1$$

$$e_2 = \frac{\alpha_1\theta_1}{1-\psi_1^2\nu_3^2}\left\{\frac{n^2}{m}\gamma^2\beta + \frac{1-\psi_1\nu_3}{2}m\beta\right\} + d_3; \quad f_1 = -d_1$$

$$f_2 = \frac{1}{1-\nu_3^2}\left\{m\beta + \frac{1-\nu_3}{2}\gamma^2\beta\frac{n^2}{m}\right\} + d_3; \quad f_3 = \frac{n\beta\gamma}{2(1-\nu_3)}$$

$$g_1 = -e_1; \quad g_2 = \frac{1}{1-\nu_3^2}\left\{\frac{n^2}{m}\gamma^2\beta + \frac{1-\nu_3}{2}m\beta\right\} + d_3$$

$$h_1 = m^3\beta^3\left[\frac{1}{12}\left\{\frac{\alpha_1\theta_1^3}{1-\psi_1^2\nu_3^2} + \frac{1}{1-\nu_3^2}\right\}\left\{1 + 2\gamma^2\left(\frac{n}{m}\right)^2 + \left(\frac{n}{m}\gamma\right)^4\right\} + \frac{\theta_2\delta_2}{m^2\beta^2}\left\{1 + \left(\frac{n}{m}\gamma\right)^2\right\}\left\{1 + \frac{1+\theta_1}{2\theta_2}\right\}^2\right] - \frac{\lambda}{m\beta}\left(\theta_1 + \theta_2\frac{\gamma_2}{\gamma_1} + \frac{1}{\gamma_1}\right) - mK_x$$

$$\theta_i = \frac{t_i}{t_3}(i = 1,3); \quad \alpha_1 = \frac{E_1}{E_3}; \quad \psi_1 = \frac{\nu_1}{\nu_3}; \quad \delta_2 = \frac{G_2}{E_3}; \quad \gamma = \frac{a}{b}$$

$$\beta = \frac{\pi t_3}{a}; \quad \gamma_i = \frac{\rho_i}{\rho_3}(i = 1,2); \quad \lambda = \frac{\rho_1\omega^2 t_3^2}{E_3} \text{ and } K_x = \frac{N_x\pi}{E_3 a}$$

For the case of a nontrivial solution, the determinant of the coefficients of $U_{1mn}$, $U_{3mn}$, $V_{1mn}$, $V_{3mn}$, and $W_{mn}$ must be equal to zero. The solution of the resulting characteristic equation yields the frequencies of the plate for specific values of applied load $N_x$.

### Numerical Results and Discussion

Plots showing the variation of $\lambda/\lambda_s$ with respect to $K_x/(K_x)_{cr}$ are presented in Figs. 2–5. These are drawn with the following values of the parameters:

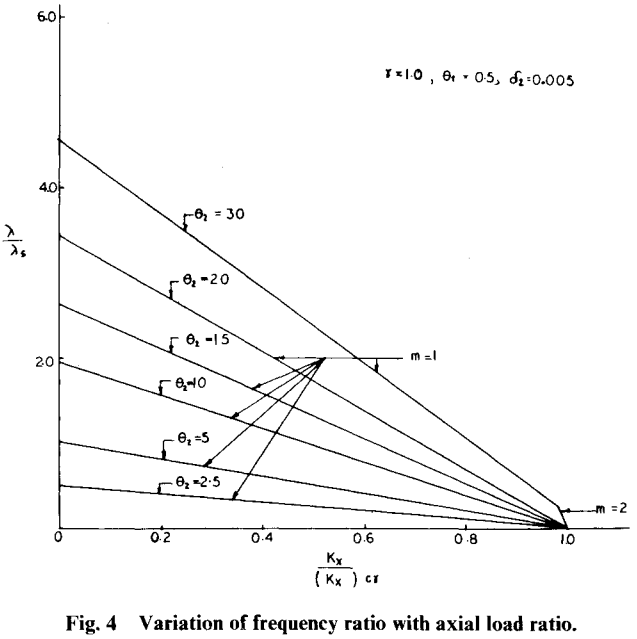


**Fig. 4 Variation of frequency ratio with axial load ratio.**

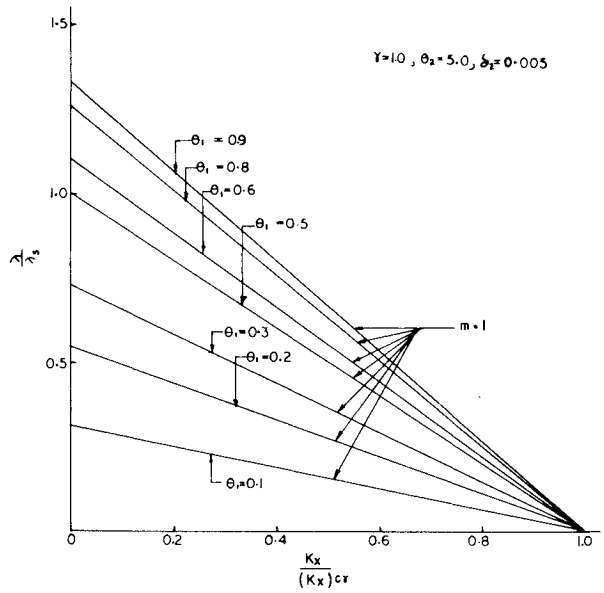


**Fig. 5 Variation of frequency ratio with axial load ratio.**

$\alpha_1 = 1.0$, $\psi_1 = 1.0$, $\nu_3 = 0.3$, $\gamma_1 = 1.0$, $\gamma_2 = 0.5$, $\beta = 0.0125$

The value of $\lambda_s$, the magnitude of which is $0.268 \times 10^{-6}$, corresponds to the frequency of an unsymmetrical square sandwich plate with $\theta_1 = 0.5$, $\theta_2 = 5.0$, and $\delta_2 = 0.005$, in addition to the preceding values of parameters. $(K_x)_{cr}$ is the nondimensional critical load of the plate under consideration. The other parameters listed in Figs. 2–5 are chosen so as to clearly point out the effect of axial load on the frequencies and on the modal pattern of the sandwich plate.

The influence of uniaxial compression on the frequencies can be observed in all cases as shown in Figs. 2–5. The frequencies are greatly reduced with the increase in axial loads and finally become zero at those corresponding to the buckling loads of the plates. It is also observed that the vibrational modes vary in the vicinity of the buckling load. From Fig. 2, it is seen that the modal patterns are affected when the aspect ratio $\gamma$ is greater than 1. At $\gamma = 4$, the value of $m$ is found to be as high as 8 just prior to buckling, unlike the case of homogeneous plates.[5] This sort of behavior can mainly be attributed to the shear deformation of the core.[6] For the case of a square plate with a weak core, it can be seen from Fig. 3 that the lowest frequencies correspond to $m = 2$ in the vicinity of the buckling load. Similar observation can also be made for a square plate having sufficiently thick core, as shown in Fig. 4. However, it is to be pointed out that the asymmetry of the faces has no influence on the modal number $m$ for a particular sandwich plate. This can be seen from Fig. 5.

## Conclusions

Free vibration analysis of unsymmetrical sandwich plates under uniaxial compression has been presented in this Note. It is shown that the frequencies and vibrational modes are greatly influenced depending upon the material and geometrical properties of the plate. This effect is found to be more predominant when the axial load approaches the critical value.

## References

[1] Habip, L. M., "A Survey of Modern Developments in the Analysis of Sandwich Structures," *Applied Mechanics Reviews*, Vol. 18, No. 2, Feb. 1965, pp. 93–98.

[2] Hoff, N. J., "Bending and Buckling of Rectangular Sandwich Plates," TN 2225, 1950, NACA.

[3] Rao, Y. V. K. S. and Nakra, B. C., "Vibratory Bending of Unsymmetric Sandwich Plates," *Archives of Mechanics*, Vol. 25, No. 2, 1973, pp. 213–225.

[4] Shahin, R. M., "Free Vibrations of Multilayer Sandwich Plates in the Presence of Inplane Loads," *The Journal of Astronautical Sciences*, Vol. XIX, No. 36, May–June, 1972, pp. 433–447.

[5] Herrmann, G., "The Influence of Initial Stress on the Dynamic Behavior of Elastic and Viscoelastic Plates," *Publications of the International Association for Bridge and Structural Engineering*, Vol. 16, 1956, pp. 275–294.

[6] Plantema, F. J., *Sandwich Construction*, Wiley, New York, 1966.

# Evaluation of a Wedge Gas-Sampling Probe

H. Lee Beach Jr.*
*NASA Langley Research Center, Hampton, Va.*

## Introduction

Gas sample profiles transverse to the main flow direction can be obtained quite successfully in many high temperature mixing and reacting flowfields with water-cooled, multiple probe rakes similar to that described in Ref. 1. The size and spacing of the probes in such a rake are determined not only by the physical dimensions of the flowfield, but also by the cooling required and consideration of interference effects between the probes. In small-scale flowfields, the combination of these constraints can make fabrication extremely costly if feasible at all. For example, scaling the probe rake described in Ref. 1 (probe diameter = 0.65 cm, spacing = 1.9 cm) for use in a flow 2.5 cm wide would require unrealistically small probe diameters of 0.11 cm with a spacing of 0.3 cm. A composition profile can be obtained, of course, by stepping a single probe of the Ref. 1 type transverse to the flow; however, this approach is not feasible for many applications due to test duration limitations.

Two alternative techniques suitable for small-scale flows are discussed in Ref. 2. One is a blunt leading edge wedge probe with multiple stagnation ports on the leading edge; the other is a sharp leading edge wedge probe with static sampling ports on the wedge surface. The attractive features of these probes are the potential for locating sampling ports very close together and the relatively simple fabrication and cooling. Substantially different results were obtained with the stagnation and static wedge probes in the supersonic mixing/reacting flow described in Ref. 2. Temperature and pressure rises associated with the detached bow shock ahead of the blunt leading edge of the stagnation probe were found to significantly alter the reaction kinetics relative to those of the static probe which had its sampling surface aligned with the flow. Another potential problem with the blunt-edged probe exists even when kinetics are not important. If the flow approaching the shock is nonuniform (in Mach number, concentration, flow direction), the relative streamline orientations behind the shock may be different from those ahead of the shock. Samples entering the stagnation ports will therefore misrepresent the undisturbed spacing of the flow in line with the ports. This is not expected to be a problem with the wedge-static probe.

To determine the acceptability of a probe similar to the static-sampling wedge probe of Ref. 2 in a small-scale flow (region of interest, 1.9 cm) pertinent to supersonic combustion ramjet research, a wedge probe has been designed, fabricated

Received January 18, 1974; revision received March 13, 1974.
Index categories: Airbreathing Propulsion, Hypersonic; Combustion in Gases.

* Aerospace Technologist, Combustion Section, Hypersonic Vehicles Division.